SANDIA REPORT

SAND87—0962 • UC—28
Unlimited Release
Printed June 1987

Beamline Considerations for a Compact, High Current, High Power Linear RF Electron Accelerator

Barry Marder

Prepared by
Sandia National Laboratories
Albuquerque, New Mexico 87185 and Livermore, California 94550
for the United States Department of Energy
under Contract DE-AC04-76DP00789

When printing a copy of any digitized SAND Report, you are required to update the markings to current standards.

SF2900Q(8-81)

Issued by Sandia National Laboratories, operated for the United States Department of Energy by Sandia Corporation.

NOTICE: This report was prepared as an account of work sponsored by an agency of the United States Government. Neither the United States Government nor any agency thereof, nor any of their employees, nor any of their contractors, subcontractors, or their employees, makes any warranty, express or implied, or assumes any legal liability or responsibility for the accuracy, completeness, or usefulness of any information, apparatus, product, or process disclosed, or represents that its use would not infringe privately owned rights. Reference herein to any specific commercial product, process, or service by trade name, trademark, manufacturer, or otherwise, does not necessarily constitute or imply its endorsement, recommendation, or favoring by the United States Government, any agency thereof or any of their contractors or subcontractors. The views and opinions expressed herein do not necessarily state or reflect those of the United States Government, any agency thereof or any of their contractors or subcontractors.

Printed in the United States of America
Available from
National Technical Information Service
U.S. Department of Commerce
5285 Port Royal Road
Springfield, VA 22161

NTIS price codes
Printed copy: A03
Microfiche copy: A01

Distribution
Category UC-28

SAND87-0962
Unlimited Release
Printed June 1987

BEAMLINE CONSIDERATIONS FOR A COMPACT, HIGH CURRENT, HIGH POWER LINEAR RF ELECTRON ACCELERATOR

Barry Marder
Plasma Theory Division 1241
Sandia National Laboratories
Albuquerque, NM 87185

ABSTRACT

A design for a compact, high current, high power linear electron accelerator using an RF power source is investigated. It consists of adjacent cavities into which RF power is injected and through which electron pulses pass. The source is assumed to be capable of delivering sufficient RF power to the desired location at the proper phase. Beamline issues such as cavity loading, energy extraction, longitudinal and transverse pulse focusing, and beam breakup are considered. A device which, given the required source, can deliver beam parameters comparable to existing induction accelerators but which is more than an order of magnitude smaller appears feasible.

CONTENTS

1. Introduction
2. Basic Design
3. Cavity Loading
4. Energy Extraction From Cavities
5. Pulse Focusing
6. Beam Breakup Instabilities
7. Accelerator Design
8. Conclusions

1. Introduction

The idea of utilizing RF electromagnetic energy to accelerate electrons to a Gev of energy dates back to the 40's.[1] The promise of new high power, long duration microwave sources, such as the magnetically insulated transmission line oscillator (MILO),[2] has generated renewed interest in some of these basic ideas. In this paper we examine the beamline considerations for the design of a compact accelerator. We shall simply assume that RF power is delivered to the accelerator at the desired location and in the required phase. While this in itself represents a formidable task, we shall not address it in any detail. Our purpose is rather to examine the possibilities and limitations of a particular RF accelerator given an ideal source. Where deviations from ideal are necessary, it should be possible to estimate the penalty paid.

In the following section we propose an accelerator concept on which to base our analysis. In doing so we do not mean to suggest that other accelerator concepts harnessing RF power would not be feasible and, indeed, there are other candidates.[3,4] The next four sections develop the tools necessary to assess the feasibility of the concept.

The third section contains our considerations of how a relativistic electron pulse interacts with a resonant structure. The passage of a pulse "loads" a cavity with electric and magnetic fields. In addition to extracting energy from the pulse, these wake-fields can influence both the beam electrons in the cavity and those on subsequent pulses.

In section four we determine the conditions under which a beam can extract energy from the electric field in a cavity.

The fifth section has an examination of the problem of beam focusing: overcoming the self electrostatic repulsion and keeping the pulses intact both longitudinally and transversely as they pass through the device.

In the sixth section we look at beam breakup. This well known instability would appear to be devastating in a small, high current accelerator. There are, however, ways to diminish its magnitude and we shall examine their effectiveness.

In the seventh section we utilize these results to examine the potential utility and fundamental limitations of this type accelerator for specific parameters. In particular, an optimized accelerator design is proposed.

The last section summarizes our findings.

2. Design Considerations

Referring to Fig. 1, the fundamental unit of our accelerator will be a resonant cavity, either rectangular with sides X and Y or cylindrical with radius R. In both cases the depth, Z, will be very much the smaller dimension. RF energy at the fundamental cavity mode is injected to maintain an oscillating electric field in the z direction. Properly phased pulses of electrons pass through a centered hole and are accelerated by the electric field in the cavity. A substantial part of our analysis will consist of examining electrical properties of these cavities: the resonant modes they support, the interaction of a cavity with an electron pulse, and the effect of energy loss in the cavity.

We shall be interested in z-independent modes with longitudinal electric field and transverse magnetic field relative to the beam propagation direction. The fundamental mode consists of an oscillating electric field with peak amplitude at the beamline and a magnetic field which vanishes at the center and loops around the cavity. Clearly, the time during which electrons can be accelerated by this field is limited to that half period during which the oscillation has the proper sign. The kinematics of a pulse passing through a cavity are shown in Fig. 2. We shall assume the pulse length is much greater than the cavity depth, $L_p >> Z$, so that the time during which part of the pulse occupies the cavity, $T_p = T_4 - T_1$, is approximately equal to the time needed for a relativistic beam to pass a single point, L_p/c. Time will be defined as starting when the pulse enters the cavity, so $T_1 = 0$.

The accelerator, then, consists of a series of adjacent cavities into which RF energy at the frequency of the fundamental mode is injected. The phase of the electric field in each cavity is such that the field delivers energy to the electrons. Such a device is characterized by the following list of parameters.

Cavity parameters:

λ_o , the fundamental mode of the cavity

ω_{λ_o}, the angular frequency of the fundamental mode

ϕ , the phase of the RF field in the cavity

W , the aspect ratio of a rectangular cavity, X/Y

Z , the depth of the cavity (in the direction of beam propagation)

Q , the quality factor of the cavity

N , the number of cavities

L , the minimum length of the accelerator (= NZ)

B_{zo}, the applied longitudinal focusing magnetic field

Pulse parameters:

b , the pulse shape factor (rise time)

T_p , the time during which the pulse occupies a cavity

I_p , the current in the pulse

ΔU_p, the energy gained by the pulse per cavity

L_p , the length of the pulse

r_p , the radius of the pulse

Derived parameters:

F , the fundamental frequency = $\omega_{\lambda_o}/2\pi$

Γ , the fundamental period of oscillation = 1 / F

X , the height of a rectangular cavity with fundamental frequency F

Y , the width of a rectangular cavity with fundamental frequency F

R , the radius of a cylindrical cavity with fundamental frequency F

d , the fraction of time the pulse is in the cavity (duty cycle)

I_{av}, the average current = dI_p

3. Cavity Loading

As a pulse of electrons passes through a cavity it excites the resonant modes of the cavity. Referring again to Fig. 1, let the cavity be pierced at location x_p by a relativistic electron pulse of length L_p and radius r_p, carrying current I_p. Assume the charge density, ρ, is independent of both r and Θ and is given by $h(s)I_p/c\pi r_p^2$ where

$$h(s) = \begin{cases} s/[L_p b(1-b)] & 0 \le s < L_p b \\ 1/(1-b) & L_p b \le s < L_p(1-b) \\ (L_p - s)/[L_p b(1-b)] & L_p(1-b) \le s \le L_p \end{cases}, \quad (1)$$

where s is the distance from the head of the pulse. This double ramped shape is illustrated in Fig. 3. The average value of h(s) in the interval 0 to L_p is 1. The current density in the z direction is given by

$$J(\mathbf{x},t) = \begin{cases} h(ct)\, I_p/\pi r_p^2 & \text{for} \quad |\mathbf{x} - \mathbf{x}_p| \le r_p \\ 0 & \phantom{\text{for}} \quad |\mathbf{x} - \mathbf{x}_p| < r_p \end{cases} . \quad (2)$$

Our analysis is similar to that used by Faehl, Lemons, and Thode[5] in which electromagnetic fields produced by the current are expressed in terms of the scalar and vector potentials,

$$\begin{aligned} \mathbf{B} &= \text{curl } \mathbf{A} \\ \mathbf{E} &= \nabla\phi - \partial \mathbf{A}/\partial t \end{aligned} , \quad (3)$$

which satisfy

$$\begin{aligned} (1/c^2)\, \partial^2\mathbf{A}/\partial t^2 - \nabla^2\mathbf{A} &= \mu\mathbf{J} + (1/c)\, \partial/\partial t\, \nabla\phi \\ \nabla^2\phi - (\partial/\partial t)\, \nabla \cdot \mathbf{A} &= \rho/\varepsilon \end{aligned} , \quad (4)$$

where c, ε, and μ have their usual meanings. We shall use the Coulomb gauge, $\nabla \cdot \mathbf{A} = 0$.

Only the z component of **A**, designated by A, is required. To solve (4), A is expressed as a sum of the orthonormal cavity eigenmodes.

$$A(\mathbf{x},t) = \sum_\lambda q_\lambda(t)\, a_\lambda(\mathbf{x}) \quad , \quad (5)$$

where λ represents ℓ and m, the indices of the mode. The eigenmodes, $a_\lambda(\mathbf{x})$, vanish on the boundary and satisfy

$$\nabla^2 a_\lambda + (\omega_\lambda/c)^2 a_\lambda = 0 \qquad \text{with} \qquad \int a_\lambda a_\nu dV = \delta_{\lambda\nu} \quad . \tag{6}$$

$\delta_{\lambda\nu}$ is the Kronecker delta which equals 1 when the indices are the same and 0 otherwise. For rectangular and cylindrical coordinates these are

$$a_{\ell m}(x,y) = 2(XYZ)^{-1/2} \sin(\ell\pi x/X) \sin(m\pi y/Y) \quad , \tag{7}$$

$$\omega_{\ell m} = c\pi \, [(\ell/X)^2 + (m/Y)^2]^{1/2} \quad , \tag{8}$$

and

$$a_{\ell m}(r,\theta) = (2/\pi Z)^{1/2} J_\ell(\omega_{\ell m} r/c) \cos(\ell\theta) \; / \; R J_{\ell+1}(\omega_{\ell m} R/c) \quad , \tag{9}$$

$$J_\ell(\omega_{\ell m} R/c) = 0 \quad . \tag{10}$$

The time-dependent coefficients in (5), $q_\lambda(t)$, satisfy the equation

$$\ddot{q}_\lambda{}^2 + \omega_\lambda{}^2 q_\lambda = (1/\varepsilon) \int a_\lambda(\mathbf{x}) \, (J + (1/\mu c) \, \partial/\partial t \, \nabla\phi) \, dV \quad , \tag{11}$$

where $\cdot$ denotes differentiation with respect to time. Using the fact that the scalar potential is zero on the boundary, it can be shown that the term in the integral containing it vanishes. With the requirements that q and its derivative are initially zero, this equation can be solved to yield:

$$q_\lambda(t) = (I_p Z/\omega_\lambda \varepsilon) \, a_\lambda(\mathbf{x}_p) \int_0^t h(c\tau) \sin(\omega_\lambda(t - \tau)) \, d\tau \quad . \tag{12}$$

The electromagnetic fields produced in the cavity by the electron pulse are, according to (3),

$$E_z(x,t) = -\sum_\lambda \dot{q}_\lambda(t)\, a_\lambda(x)$$

$$B(x,t) = \sum_\lambda q_\lambda(t)\, (\nabla \times a_\lambda(x) e_z) \quad . \tag{13}$$

Figure 4 depicts the beamline electric field produced by a centered pulse in a square cavity for b = .05, .25 and .5 as a function of s. Notice that the field amplitude in (13) depends on the beam intersect location, x_p, occurring in $q_\lambda(t)$. The energy in each mode, U_λ, is given by

$$U_\lambda = (\varepsilon/2)\, (\dot{q}_\lambda^{\,2} + \omega_\lambda^{\,2} q_\lambda^{\,2}) \quad . \tag{14}$$

4. Energy Extraction from Cavities

In this section we investigate the extraction of energy by a pulse from the fundamental mode of a cavity. Assume the electric field in the empty cavity is

$$E_{cav}(x,t) = E_{rf}\, \sin(\omega_{\lambda_o} t + \phi)\, a_{\lambda_o}(x) \,/\, a_{\lambda_o}(x_c) \quad , \tag{15}$$

where λ_o represents the fundamental mode of the cavity, either $\ell = m = 1$ for a rectangular cavity or $\ell = 0$, $m = 1$ for a cylindrical one. x_c is the cavity center and E_{rf} is the peak amplitude of the applied RF field. Associated with this electric field is a $q_{rf}(t)$ defined by (13):

$$q_{rf}(t) = E_{rf}\, \cos(\omega_{\lambda_o} t + \phi) \,/\, \omega_{\lambda_o} a_{\lambda_o}(x_c) \quad . \tag{16}$$

The energy in the cavity before the pulse enters is

$$U_{rf} = (\varepsilon/2)\, (\dot{q}_{rf}^{\,2} + \omega_{\lambda_o}^{\,2} q_{rf}^{\,2}) \quad . \tag{17}$$

The energy remaining in the fundamental mode after passage of the pulse is

$$U_{fin} = (\varepsilon/2)\, [(\dot{q}_{rf} - \dot{q}_{\lambda_o})^2 + \omega_{\lambda_o}^{\,2} (q_{rf} - q_{\lambda_o})^2] \quad . \tag{18}$$

The pulse also excites higher modes in the cavity which receive an amount of energy, U_{hi}, given by

$$U_{hi} = (\varepsilon/2) \sum_{\lambda \neq \lambda_o} \dot{q}_\lambda^{\,2} + \omega_\lambda^{\,2} q_\lambda^{\,2} \quad . \tag{19}$$

The net energy gained by the pulse, U_p, is equal to the energy change of the fundamental mode minus the energy injected into higher modes.

$$\begin{aligned} U_p &= U_{rf} - U_{fin} - U_{hi} \\ &= (\varepsilon/2)\ [2\ (\dot{q}_{rf}\dot{q}_{\lambda_o} + \omega_{\lambda_o}^{\,2} q_{rf} q_{\lambda_o}\ ) - \sum_\lambda (\dot{q}_\lambda^{\,2} + \omega_\lambda^{\,2} q_\lambda^{\,2})] \quad . \end{aligned} \tag{20}$$

The energy remaining in a cavity after the passage of a pulse will be dissipated by various loss mechanisms represented by the cavity quality factor, Q. The energy in the fundamental mode which is lost to the cavity in one period is approximately

$$U_{loss} = (1 - e^{-2\pi/Q}) U_{fin} \quad . \tag{21}$$

In order to achieve steady state operation, the energy fed into the cavity during each cycle must be sufficient to restore the fundamental mode to its initial strength. The required input energy is, therefore,

$$U_{in} = U_{rf} - U_{fin} + U_{loss} = U_{rf} - U_{fin} e^{-2\pi/Q} \quad . \tag{22}$$

The efficiency, defined as the ratio of the energy gained by the pulse to the input energy per period during steady state operation, is

$$\eta = U_p/U_{in} = U_p/(U_{rf} - U_{fin} e^{-2\pi/Q}) \quad . \tag{23}$$

The fields in the cavities after multiple pulses consist of a mixture of modes. With the exception of the fundamental, which is replenished each period, the modes oscillate at different frequencies and dissipate at different rates. We have, therefore, treated each cavity as if it were initially free of fields, making the assumption that, on the average, these higher modes do not influence the pulses.

The discussion so far has been for pulses with arbitrary shape. For the remainder of this section let us assume the pulses have constant density throughout their length, that is, b = 0. This will provide an estimate of the energy transfer between pulse and cavity. With this shape pulse we find that for $t > T_p$, (12) becomes

$$q_\lambda(t) = (2I_pZ/\varepsilon\omega_\lambda^2)\, a_\lambda(x_p)\, \sin(\omega_\lambda T_p/2)\, \sin(\omega_\lambda(t - T_p/2)) \quad . \tag{24}$$

Utilizing (20) and replacing T_p by $2\pi d/\omega_{\lambda_o}$, we obtain

$$U_p = 2\, I_pZ\, \sin(\pi d)\, \sin(\pi d + \phi)\, (E_{rf} - E_{min})/\, \omega_{\lambda_o} \quad , \tag{25}$$

where

$$E_{min} = \kappa\, I_pZ\, a_\lambda(x_p)^2\, \sin(\pi d)\, /\, (\varepsilon\omega_{\lambda_o} \sin(\pi d + \phi)) \quad , \tag{26}$$

and

$$\kappa = \sum_\lambda [a_\lambda(x_p)\omega_{\lambda_o} \sin(\pi d\omega_\lambda/\omega_{\lambda_o})/a_{\lambda_o}(x_p)\omega_\lambda \sin(\pi d)]^2 \quad . \tag{27}$$

E_{min} is the magnitude of the minimum RF electric field necessary to impart energy to the pulse. κ is a measure of the electromagnetic energy loaded into a cavity by the passage of a pulse. It is a function of the location where the pulse pierces the cavity, the duty cycle, and the shape of the cavity. Assuming a rectangular cavity pierced at its center, we obtain

$$\kappa = \sum_{\ell,m \text{ odd}} [\omega_{11} \sin(\pi d\omega_{\ell m}/\omega_{11})/\omega_{\ell m} \sin(\pi d)]^2 \quad . \tag{28}$$

For the cylindrical case, only $\ell = 0$ modes contribute:

$$\kappa = \sum_m [J_1(\omega_{01}R/c)\omega_{01}\sin(\pi d\omega_{0m}/\omega_{01})/J_1(\omega_{0m}R/c)\omega_{0m}\sin(\pi d)]^2 \quad . \tag{29}$$

Plots of κ vs. d are given in Fig. 5 for cylindrical and rectangular cavities. Letting $\xi = E_{min}/E_{rf}$, the efficiency, (23), can be written

$$\eta = 4\kappa\xi(1 - \xi)\sin^2(\pi d + \phi)/\{\kappa^2 - e^{-2\pi/Q}[\kappa^2 + 4\xi(\xi - \kappa)\sin^2(\pi d + \phi)]\} \quad . \tag{30}$$

As an interesting aside, we can determine the fraction of energy a single pulse can extract from the fundamental mode of a resonating cavity. This is the energy extracted by the pulse, minus the energy loaded into the cavity, divided by the original energy in the cavity. To obtain this, let $Q = 0$ in (30) so that all the energy remaining in the cavity after passage of the single pulse is lost:

$$\eta_s = 4\xi(1 - \xi)/\kappa \sin^2(\pi d + \phi) \quad . \tag{31}$$

This attains a maximum value of $\sin^2(\pi d + \phi)/\kappa$ when $\xi = 1/2$ (i.e., $E_{rf} = 2\,E_{min}$). From Fig. 5 we see, for example, that the maximum single pulse extraction efficiency for a cylindrical cavity is about 50%, for a square cavity it is about 40%, and it decreases as the cavity elongates.

If we assume the energy in electron volts gained by the pulse in each cavity is $\Delta U_p[ev]$, the power fed to the pulse is

$$I_p\ \Delta U_p[ev] = U_p/T_p \quad . \tag{32}$$

Using (25), substituting $2\pi d/\omega_{\lambda_o}$ for T_p, and L for NZ, we obtain the total energy gain in N cavities:

$$\Delta U[ev] = N\ \Delta U_p[ev] = L \sin(\pi d)\sin(\pi d + \phi)\ (E_{rf} - E_{min})/\pi d \quad . \tag{33}$$

Alternatively, this expression can be used to find the minimum length of an accelerator capable of imparting a given energy to a pulse.

5. Pulse Focusing

As the pulse passes through the accelerator it will experience both radial and longitudinal forces produced by its own space charge. The requirement that the pulse remain intact during its transit of the accelerator places constraints on the design.

The radial expansion can be approximated by assuming a sharp edged pulse and following the boundary in time. Assuming the beam has no net canonical angular momentum, its motion will be governed by[6]

$$d/dt\ (\gamma dr/dt) - \gamma v_\theta^2/r = (e/m)\ (E_r + v_\theta B_z - v_z B_\theta) \quad , \tag{34}$$

$$\gamma r v_\theta - (e/2m)\ B_z r^2 = 0 \quad . \tag{35}$$

The longitudinal magnetic field, B_z, consists of the applied field, B_{zo}, and the diamagnetic field arising from the beam's own rotation.[7] The latter field is, in general, far smaller than the applied field and its effect on the motion will be ignored. Defining $\Omega = eB_{zo}/m$ yields

$$d/dt\ (\gamma dr/dt) + \Omega^2 r/4\gamma = eI_p/(2m\varepsilon c\pi\beta\gamma^2 r) \quad , \tag{36}$$

where we have used $E_r = I_p/2\pi\varepsilon cr$ and $B_\theta = \beta E_r/c$, the surface values obtained for an infinite uniform cylindrical beam. Here m is the electron mass, β is the electron velocity divided by the speed of light, and $\gamma^2(1 - \beta^2) = 1$. Both β and γ are functions of time. The applied magnetic field for which the pulse radius remains unchanged is

$$B_{zo} = (1/r_p)(2I_p m/\gamma\varepsilon\pi ec\beta)^{1/2} \quad . \tag{37}$$

Pulses are also subject to longitudinal forces produced by a combination of the electrostatic and inductive electric fields. Consider a pulse of radius r_p and length L_p carrying a current I_p in a cylinder of radius R_c. When Maxwell's equations are transformed into the pulse frame by defining $\zeta = z - vt$ the steady-state equations for the electric fields are

$$E_z = \gamma^{-2}\partial\psi/\partial\zeta \ , \tag{38}$$

and

$$E_r = \partial\psi/\partial r \ , \tag{39}$$

where ψ satisfies

$$r^{-1}\partial/\partial r(r\partial\psi/\partial r) + \gamma^{-2}\ \partial^2\psi/\partial\zeta^2 = \rho/\varepsilon \ , \tag{40}$$

with $\psi = 0$ on the outer wall. It is clear from (40) that as γ increases, the dependence of ψ on ζ becomes weaker, diminishing the value of E_z. It is further reduced by another factor of γ^2 occurring in (38). The results of solving this equation numerically bear this out. For a duty cycle of 1/2 and a shape factor of .25, the resultant field is illustrated in Fig. 6 for a range of γ. When the beam is weakly relativistic ($\gamma \approx 2$), the electric field is predominantly electrostatic. This causes the head of the pulse to be accelerated and the tail to be decelerated. As the energy of the pulse increases, however, the inductive electric field gains in strength with a sign opposite the electrostatic field. For $\gamma = 8$ (3.6 Mev) the resultant longitudinal field essentially vanishes. It appears, therefore, that in a high energy electron accelerator, longitudinal defocusing of the pulses will not be a problem where the pulses become even modestly relativistic. Furthermore, when it becomes relativistic, its velocity cannot significantly increase, only its energy. Thus, an applied electric field cannot "overfocus" a pulse and cause it to shorten.

6. Beam Breakup Instabilities

Modes with one even and one odd index in rectangular cavities, or modes with $\ell = 1$ in a cylindrical cavity, can interact with pulses through the magnetic field at the center of the cavity. Figure 7 sketches the magnetic field in a rectangular cavity for the 21, 41, 23, and 43 modes as well as the 10, 11, and 12 modes in a cylindrical cavity. This transverse magnetic field can divert electrons as they transit the cavity. As (13) shows, these modes are created only when the pulse crosses the cavity off-center. That is, to create a 21 mode in a rectangular cavity, a pulse must pass either to the right or left of center. Some nimble employment of the

right hand rule will demonstrate that the magnetic field created by passage to the right of center has the effect of creating a magnetic field which diverts the next pulse even further in that direction. This is the origin of the beam breakup instability.[8] It is amplified by high currents, small cavities (i.e., high frequency), high Q, long total length, and a large number of pulses. We can do nothing about the high current or the number of pulses if we desire a high power, long pulse duration accelerator and we must live with small cavities if the device is to be "compact". As we shall see, however, we can reduce the effective length with respect to the instability without reducing the actual accelerating length.

Let us consider breakup due to the ℓm mode in a rectangular cavity. Assume the beam does not move vertically, but remains centered at $y_p = Y/2$. From (13) we obtain for the y component of the magnetic field

$$B_{y\ell m} = (8\ell\pi I_p/\varepsilon\omega_{\ell m}{}^2X^2Y)\ \sin(\ell\pi x_p/X)\ \cos(\ell\pi x/X)$$
$$\sin(\pi d\omega_{\ell m}/\omega_{11})\ \sin(\omega_{\ell m}(t - \pi d/\omega_{11})) \quad . \tag{41}$$

Notice that this field has its peak amplitude at the center of the cavity and is created only when x_p is not equal to X/2. Beam breakup can be studied numerically in the following manner. The time dependent term in (41) is taken to be 1, giving a worst case approximation. Assuming the cavities are labeled with n and the pulses are numbered by k, the field in cavity n after passage of pulse k will be denoted by B(n,k). This field acts on pulses subsequent to k. During the time a relativistic pulse takes to cross the cavity, Z/c, it acquires a specified amount of longitudinal energy as well as being diverted by the **V** x **B** force. In addition, it loads magnetic field into the cavity according to (41). Finally, the fields in each cavity are reduced in value by $e^{-\omega_{\ell m}\Gamma/2Q}$ after each pulse.

It is not necessary to reduce the actual number of cavities in the accelerator to control beam breakup, only the "effective" number. By this we mean the number of essentially identical cavities through which the beam passes. We can do this by using several differently shaped cavities whose fundamental frequencies are equal, but for which the frequencies of the undesirable transverse magnetic modes are different from each other. That is, we shall use cavities with different cross-sections. The ratio of the

frequencies of higher modes to that of the fundamental in a rectangular cavity with $W = X / Y$ is

$$(\omega_{\ell m}/\omega_{11})^2 = (\ell^2 + m^2W^2)/(1 + W^2) \quad . \tag{42}$$

For a cylindrical cavity it is χ_{1m}/χ_{01} where $\chi_{\ell m}$ is the mth zero of the ℓth Bessel function.

In order for two cavities to be considered "distinct", the frequencies of the modes whose magnetic field lies in the same direction must be sufficiently different that they are not coupled by the cavities. This provides a bound on the frequency separation:[9]

$$\Delta\omega > \omega/Q \quad . \tag{43}$$

For larger values of Q the modes are more readily distinguished, so more distinct cavities exist. It is this possibility that suggests using rectangular cavities.

Table I gives the frequencies for a variety of rectangular cavities and the cylindrical cavity. (43) can be used to determine how many of these are "distinct" for a given Q. By spacing the similar cavities uniformly throughout the accelerator, the effective number of cavities with respect to beam breakup is lowered. Since the growth rate is a strong function of the distance that the pulse travels while subject to a particular unstable mode, this cavity distribution can significantly reduce its magnitude.

TABLE I

Rectangular Cavities

	X/Y	ω_{21}/ω_{11}	ω_{41}/ω_{11}	ω_{23}/ω_{11}	ω_{43}/ω_{11}
1	0.0	2.000	4.000	2.000	4.000
2	0.2	1.971	3.927	2.048	3.966
3	0.3	1.937	3.842	2.101	3.927
4	0.4	1.894	3.732	2.166	3.877
5	0.5	1.839	3.606	2.236	3.821
6	0.6	1.791	3.468	2.307	3.761
7	0.7	1.736	3.327	2.376	3.701
8	0.8	1.682	3.185	2.440	3.643
9	0.9	1.630	3.048	2.498	3.587
10	1.0	1.581	2.916	2.550	3.536
11	1.11	1.531	2.777	2.601	3.483
12	1.25	1.473	2.618	2.655	3.425
13	1.43	1.410	2.436	2.712	3.362
14	1.67	1.339	2.230	2.771	3.294
15	2.0	1.265	2.000	2.828	3.225
16	2.5	1.189	1.752	2.883	3.157
17	3.3	1.117	1.496	2.930	3.095
18	5.0	1.056	1.256	2.968	3.045
19	∞	1.000	1.000	3.000	3.000

Cylindrical Cavity

		ω_{11}/ω_{01}	ω_{12}/ω_{01}	ω_{13}/ω_{01}	ω_{43}/ω_{11}
20		1.593	2.917	4.231	5.540

Cavities can also be coupled through different modes. For example, in Table I the 41 mode of cavity number 10 has the value 2.916 while the 23 mode of cavity 18 has the value 2.968. When one designs an accelerator, these factors must be considered. In general, however, the growth rates of the higher modes are smaller than that of the lowest mode. For example, the magnetic fields for the 41, 23, and 43 modes are smaller than those for the 21 mode by factors of .05, .17, and .21 respectively due primarily to the influence of the $\sin(\pi d\omega_{\ell m}/\omega_{11})$ term in (41).

Let N_{dist} designate the number of cavities which can be considered distinct for a given mode and Q. We shall restrict the cavities to those with aspect ratio between 1/5 and 5, as in Table I. The average $\Delta\omega$ can be approximated by the difference in the frequency between the two extreme cavities (numbers two and eighteen) divided by the number of distinct cavities, so (43) becomes

$$\Delta\omega \simeq (\omega_{max} - \omega_{min})/N_{dist} > \omega_{max}/Q \quad . \tag{44}$$

There is another limit to the required frequency separation. It serves no purpose to have the modes appear "distinct" to the cavity if the two frequencies are so close that they appear identical during a time sufficient for the instability to develop. That is, if the beat period of the two modes is longer than the time required for the instability to develop, the two modes are essentially equivalent. This resolves the apparent paradox that, for infinite Q, there are an infinity of "distinct" cavities which differ only infinitesimally in their dimensions. Thus, a stable accelerator could be built with a large number of virtually identical, very high Q, cavities, a proposition we know to be false.

To quantify this notion, let us define N_{stab} to be the number of cavities for a particular Q through which an infinite number of pulses can pass without moving laterally more than ten times its initial displacement. In the next section we shall obtain N_{stab} for parameters of interest by using the code. Let us stipulate that in the time needed to cross N_{stab} cavities, $t = Z\, N_{stab}/c$, the two oscillations under consideration must become at least 90° out of phase:

$$\Delta\omega > \pi\, c/(2\, Z\, N_{stab}) \quad . \tag{45}$$

Using this and (44) gives the following constraints on the number of distinct cavities

$$N_{dist} < (\omega_{max} - \omega_{min}) \text{ MIN } \{Q/\omega_{max}, 2ZN_{stab}/\pi c\} \quad . \tag{46}$$

An accelerator consisting of N_{stab} blocks each of which contains N_{dist} distinct cavities will be stable to beam breakup. If, however, a longitudinal guide magnetic field is applied, the pulse will rotate as it passes through the accelerator. This could couple modes with different orientation. To avoid this, the cavities could be progressively skewed at such an angle that the pulses enter each cavity at the same orientation. The above analysis would then still be valid.

7. Accelerator Design

The following parameters characterize the accelerator performance:

I_{av}[kA], the average current,
ΔU[MeV], the exit energy of the pulse,
L[m], the length of the accelerator,
F[GHz], the frequency of the RF source,
d, the duty cycle,
ϕ, the phase of the RF cycle relative to the pulses,
W, the aspect ratio of the rectangular cavities, and
B_{max}[T], the maximum applied longitudinal magnetic field

Using the results derived in the previous sections we shall attempt to design an accelerator which is stable both to beam breakup and defocusing.

For the cavities themselves, we shall assume that the depth, Z, is one tenth the side of the square cavity (W = 1) corresponding to the chosen frequency. The following is a list of formulas for accelerator parameters accompanied by the numbers of the expressions in the text from which they were derived.

(8) => $$X[\text{cm}] = 15\ (1 + W^2)^{1/2}/F[\text{GHz}] \quad , \tag{47}$$

(8) => $$Y[\text{cm}] = X[\text{cm}]/W \quad , \tag{48}$$

$$(10) \Rightarrow \qquad R[\mathrm{cm}] = 11.48/F[\mathrm{GHz}] \quad , \tag{49}$$

$$\text{Assumption} \qquad Z[\mathrm{cm}] = 2.12/F[\mathrm{GHz}] \quad , \tag{50}$$

$$\text{Definition} \qquad N = 100\ L[\mathrm{m}]/Z[\mathrm{cm}] \quad , \tag{51}$$

$$\text{Definition} \qquad L_p[\mathrm{cm}] = 30\ d/F[\mathrm{GHz}] \quad , \tag{52}$$

$$(37) \Rightarrow \qquad r_p[\mathrm{cm}] > .117(I_{av}[\mathrm{kA}]/\gamma\beta d)^{1/2}/B_{max}[\mathrm{T}] \quad , \tag{53}$$

$$(26) \Rightarrow \quad E_{min}[\mathrm{kV/cm}] = 32 I_{av}[\mathrm{kA}]F[\mathrm{GHz}]\kappa W \sin(\pi d)/(d(1 + W^2)\sin(\pi d + \phi)) \quad , \tag{54}$$

$$(33) \Rightarrow \quad E_{rf}[\mathrm{kV/cm}] = E_{min}[\mathrm{kV/cm}] + 10\pi d\Delta U[\mathrm{MeV}]/(L[\mathrm{m}]\sin(\pi d)\sin(\pi d + \phi)) \quad , \tag{55}$$

$$(30) \Rightarrow \eta = 4\kappa\xi(1 - \xi)\sin^2(\pi d + \phi)/\{\kappa^2 - e^{-2\pi/Q}(\kappa^2 + 4\xi(\xi - \kappa)\sin^2(\pi d + \phi))\} \quad , \tag{56}$$

where $\xi = E_{min}/E_{rf}$.

The ratio Z/L_p, which equals .212 for a square cavity, marginally satisfies the criterion that the pulse length be much greater than the cavity depth.

The discussion so far has been kept as general as possible. To proceed further requires specifying some of the accelerator parameters. Let us take for the electron energy and total length the values

$$\Delta U = 20\ \mathrm{MeV} \qquad L = 4\ \mathrm{m} \quad . \tag{57}$$

As is evident from (56), for maximum efficiency, κ should be as small as possible. According to Fig. 5, this is achieved for a duty cycle of 1/2. Furthermore, the phase required for optimum efficiency is given by $\pi d + \phi = \pi/2$, giving a phase of 0. Thus, peak efficiency is achieved when part of the pulse is in the cavity for the entire duration of the accelerating electric field. Such operating conditions will not, however, produce uniform acceleration along the beam, a situation exacerbated by the influence of the wake field loaded into the cavities. As indicated in

Fig. 4, this field decelerates the head of the pulse while it supplies energy to the tail. To counter its effect, the RF field acting on the head must be larger than that on the tail. This requires that the duty cycle be less than 1/2 and the phase, ϕ, be positive. Let us take the duty cycle to be 1/3 and specify that the RF electric field should pass through zero just as the pulse exits the cavity. That is,

$$d = 1/3 \qquad \text{and} \qquad \phi = \pi/3 \quad . \tag{58}$$

Notice that this specification of the phase is opposite that for non-relativistic ion accelerators in which cavity loading effects do not enter. In these devices the electrostatic fields are not cancelled by the inductive fields and the pulses experience an expansive longitudinal force. To counteract this, the pulse must experience a rising electric field so that the tail will be accelerated more than the head.

We shall consider beam breakup with the parameters of (57) and (58). In particular, we shall use the code to determine N_{stab}, the number of cavities through which an essentially infinite number of pulses can pass without undergoing a displacement of more than 10 times the initial value. As an example of the code output, Figs. 8a, b, and c illustrate the results of in square cavities for Q = 10, 100, and ∞ and an average current of 1 kA. The plots show the displacement of the last pulse after passing through a given number of cavities vs. the number of previous pulses. It is clear that unless Q is fairly small, large numbers of pulses will not pass through many cavities for these parameters. It appears, however, that even for a Q of 100, an unlimited number of pulses can pass through 10 identical cavities without suffering excessive displacement. Repeated use of the code with different parameters suggests that N_{stab} can be approximated by

$$N_{stab} \approx 120(I_p[kA]Q)^{-1/2} \quad . \tag{59}$$

Using (46) and the frequencies for the most unstable mode in Table I, we obtain for the total number of cavities in the accelerator

$$N < N_{dist}\, N_{stab} < \mathrm{MIN}\{55.8(Q/I_p[kA])^{1/2},\ 3720/I_p[kA]Q\} \ . \tag{60}$$

Figure 9 is plots of N_{dist}, N_{stab}, and N vs Q for I_p = 3 kA (1 kA average current). The maximum N occurs when $Q = 16.6/I_p^{1/3}$. For I_p equal 3 kA this gives 108 cavities at a Q of 11.4. From the figure it is clear that, for any number of cavities below this limit, there is a range of acceptable Q. Since the efficiency increases with Q, the upper limit is preferable.

The final output parameters can be expressed as functions of the average current and frequency of the RF source. Using the parameters in (57) and (58), and taking the representative values $\kappa = 4$ and $\kappa W/(1 + W^2) = 1.5$, the expressions in (51), (55), (56), and the discussion in the preceeding paragraph imply

$$N = 188\ F[\mathrm{GHz}] \quad , \tag{61}$$

$$34\ I_{av}[\mathrm{kA}]\ F[\mathrm{GHz}]^2 < Q < 6.6/(I_{av}\ [\mathrm{kA}]\ F[\mathrm{GHz}]) \ , \tag{62}$$

$$E_{rf}[\mathrm{kV/cm}] = 144\ F[\mathrm{GHz}] + 70 \ , \tag{63}$$

$$\eta = 12\ \xi(1 - \xi)/\{16 - e^{-2\pi/Q}(16 + 3\ \xi^2 - 12\ \xi)\}\} \ , \tag{64}$$

where $\xi = \{1 + .5/F[\mathrm{GHz}]\}^{-1}$. The efficiency, (64), is plotted for these parameters as a function of frequency in Fig. 10 for several values of Q, including the region defined by (62). Notice that (62) gives a maximum frequency of the RF source for an accelerator of this type:

$$F[\mathrm{GHz}] < .6\ I_{av}[\mathrm{kA}]^{-2/3} \quad . \tag{65}$$

The radius of the pulse is related to the applied magnetic field by (53). For a pulse radius of 1 cm and an injection energy of 1 MeV the applied magnetic field at injection need be no larger than .12 Tesla. It can decrease along the device as $\gamma^{-1/2}$.

An electron pulse passing through a driven cavity is acted upon by three electric fields: the RF cavity field, (15); the wake field loaded into the cavity by the pulse, given by (13) and plotted in Fig. 4; and the self electrostatic/inductive field, given by (38) and (40). The beamline values of the first two of these fields, expressed as functions of the distance from the head of the pulse are, respectively

$$E_{cav}(s) = E_{rf} \sin(2\pi ds/L_p + \phi) \quad , \tag{66}$$

$$E_{load}(s) = (I_p Z/\varepsilon) \sum_{\lambda} a_{\lambda}^2(x_p) \int_0^{s/c} h(c\tau)\cos(\omega_{\lambda}(\tau - s/c))d\tau \quad . \tag{67}$$

The third field, as we have seen, plays almost no role for relativistic pulses. The net force on the pulse, therefore, arises from the sum of the loaded field and RF field.

Suppose the RF source has a frequency of 500 MHz and the beam has an average current of 1 kA. From (61) we see that the number of cavities in the accelerator is 94. The Q of the cavities should be about 13. This results in an efficiency of about 35% as shown in Fig. 10. The accelerator consists of 19 cavities of each of five distinct shapes. These could be, for example, the cavities numbered 2, 6, 10, 14, and 18 in Table I, which measure

30.6 by 153,
35 by 58.3,
42.4 by 42.4,
58.3 by 35, and
153 by 30.6 cm.
All cavities are 4.24 cm deep

For purposes of frequency discrimination the cylindrical cavity is indistinguishable from the square one at this Q. While there is no harm in using both of these cavities in the accelerator, little is to be gained insofar as eliminating beam breakup. The N cavities would be evenly spaced throughout the accelerator in N_{stab} groups consisting of N_{dist} cavities each, as sketched in Fig. 11. The applied RF electric field at 500 MHz has a peak amplitude of 142 kV/cm. Figure 12 is plots of the net electric field acting on a pulse with shape factor .25 for 1 kA average current.

Clearly, although the total energy given to the pulse satisfies the given conditions, the energy distribution as indicated by Fig. 12 varies considerably along the pulse. If this is unacceptable, the frequency can be reduced. This decreases the severity of the cavity loading by increasing the size of the cavities. Figure 13 shows the total electric

field resulting from a frequency of 166 MHz. E_{rf} is now only 94 kV/cm and the cavities are three times as large, while the length is still 4 meters. The energy distribution is more uniform, although still far from constant. There are now, according to (61), only 32 cavities in the device. If the Q remains at 13, the efficiency, as read from Fig. 10, falls to around 22%. With this lower frequency, however, a Q of about 40 can be used, increasing the efficiency to 40%. N_{dist} and N_{stab} for this Q are 3 and 10 respectively, so the accelerator consists essentially of 10 blocks of 3 distinct cavities each.

Another way to achieve a more uniform energy spread is to tailor the waveform of the input RF. If it is possible to add higher harmonics, the applied field can more closely match the loaded field.

The above considered RF electric fields, 142 kV/cm at 500 MHz and 94 kV/cm at 166 Mhz, are, by a considerable margin, both too large to cause electron multipactoring[6] and too small to cause sparking according to Kilpatrick's criterion.[10]

Conclusions

There are, obviously, a wide range of parameter choices available in designing an accelerator along these lines. We have attempted to provide the tools required to facilitate this design. An example was presented of an accelerator 4 meters long, and about 1.5 meters wide, which accelerates a 1 kA average current beam to 20 MeV at an efficiency of about 40%. The beam is stable both to beam breakup and defocusing forces, although if the input RF wave form is restricted to a pure sinusoid, some energy spread, which increases with frequency, is unavoidable. With this caveat, it appears that, given an RF source which can meet the stated requirements, a linear high power, high current RF electron accelerator, which is at least an order of magnitude more compact than existing induction devices, is feasible.

ACKNOWLEDGMENTS

My initial ignorance of accelerator technology was diminished by conversations with knowledgeable and patient people and I would like to thank them for their help. The Sandians among them include Bruce Miller, Collins Clark, Larry Bacon, Dale Coleman, Regan Stinnett and Ron Lipinski. Discussions with Stan Humphries and Brendan Godfrey were also quite helpful, as was Brendan's corroboration of my calculations on beam breakup. I appreciate also the time taken by Dick Cooper from LANL and Kelvin Niel of LLL who listened to my primitive notions on high power accelerators and tempered them with the voice of experience.

REFERENCES

1. E. L. Ginzton, W. W. Hansen, and W. R. Kennedy, Rev. Sci. Inst. 19, 89, (1947).
2. M. C. Clark and B. M. Marder, submitted to Phys. Rev. Letters.
3. J. Nation and S. Greenwald, Bull. Am. Phys. Soc. Vol 31, No 9, Oct., 1986.
4. M. Friedman and V. Serlin, Appl. Phys. Lett 49 (10), 596 (1986).
5. R. J. Faehl, D. S. Lemons, and L. E. Thode, Los Alamos Report LA-9126-MS, January 1982.
6. S. Humphries, Jr., Principles of Charged Particle Acceleration, (John Wiley and Sons, New York, 1986).
7. R. B. Miller, Intense Charged Particle Beams, (Plenum Press, New York, 1982).
8. W. Panofsky and M. Bander, Redv. Sci. Inst. 39, 2076 (1968).
9. B. Godfrey (private communication).
10. W. D. Kilpatrick, Rev. Sci. Inst. 28, 824 (1957).

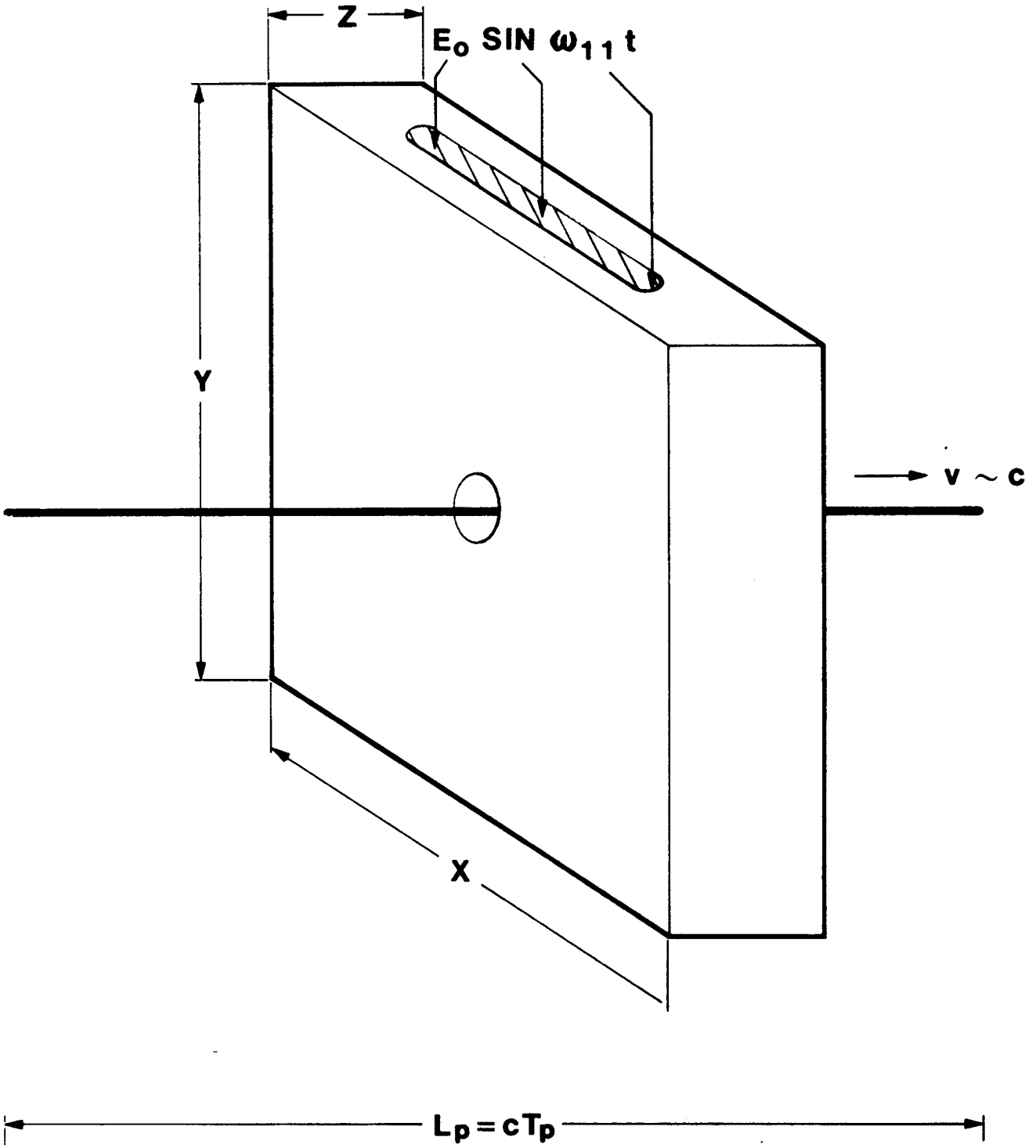

FIGURE 1. The RF cavities which form the basis of the accelerator.

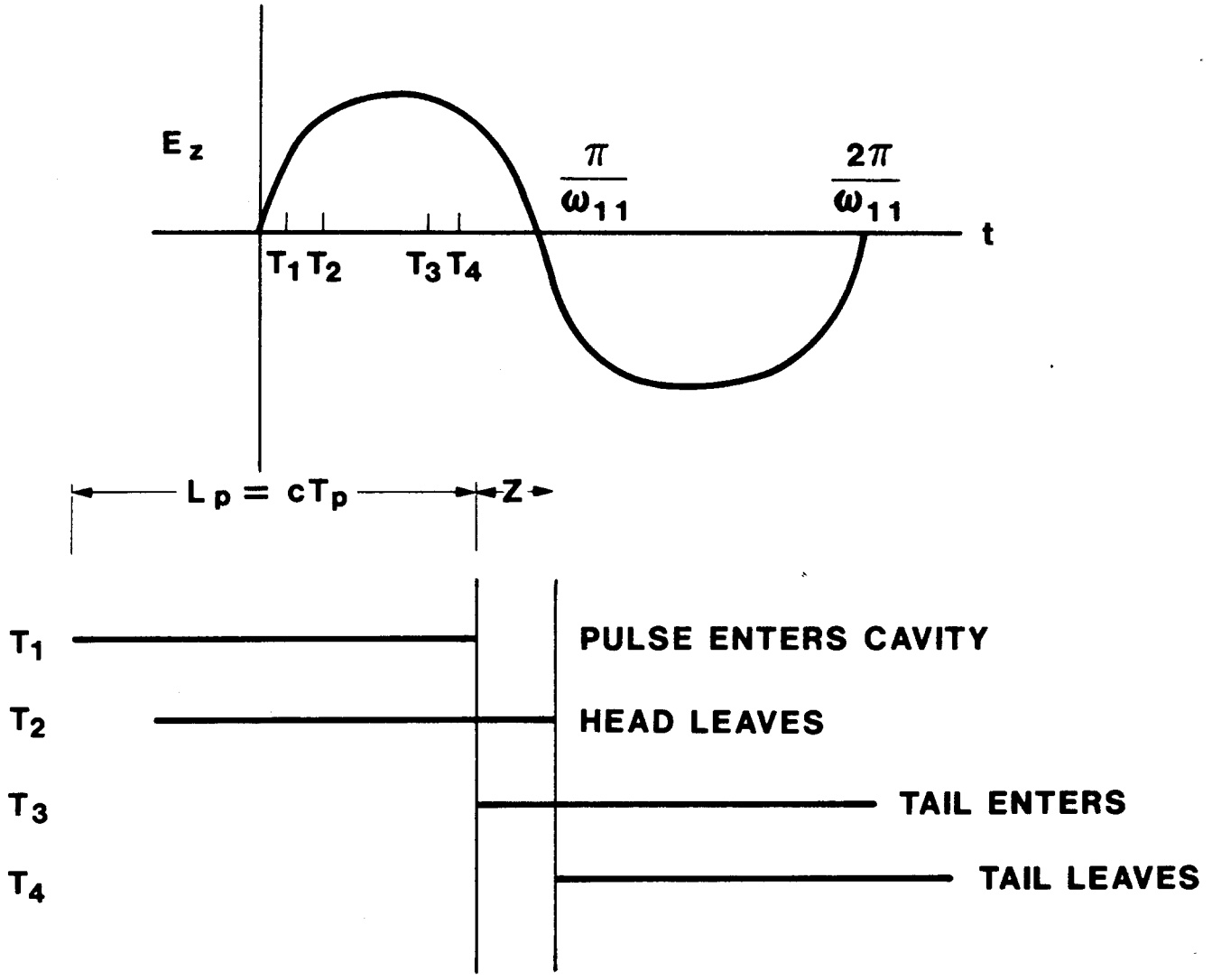

FIGURE 2. The kinematics of an electron pulse piercing a cavity.

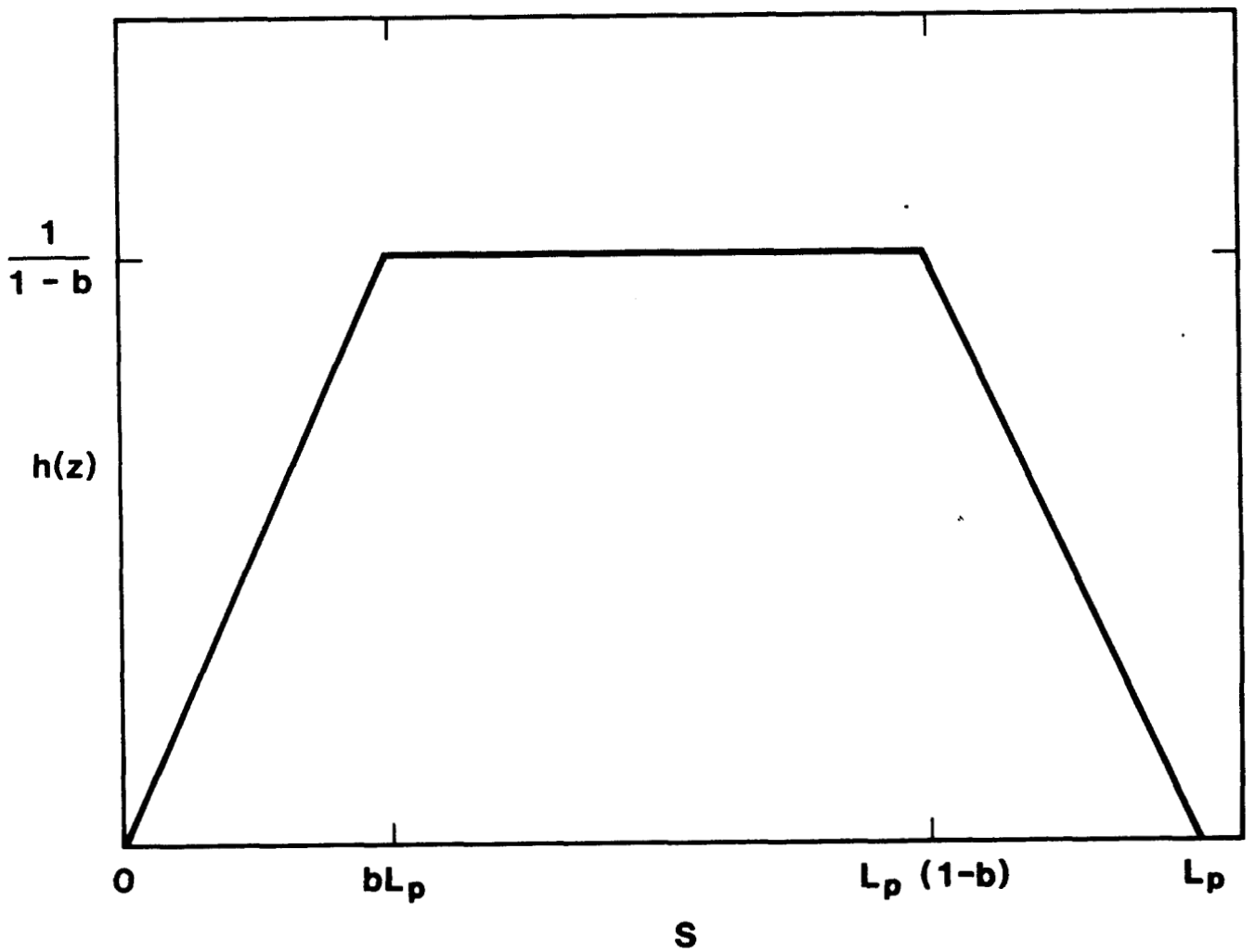

FIGURE 3. The pulse shape as parameterized by b.

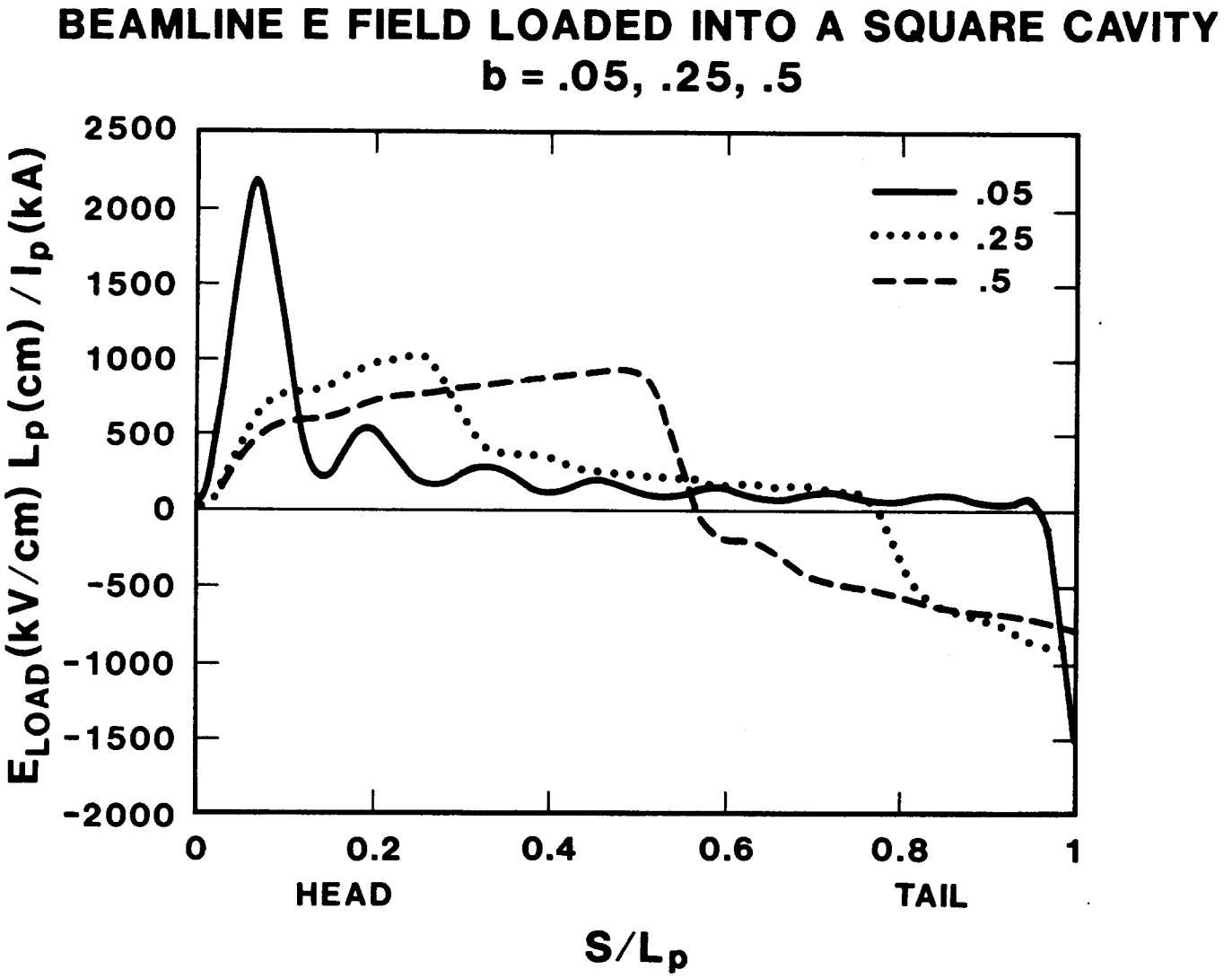

FIGURE 4. Beamline electric field loaded into a square cavity for pulse shapes given by b = .25 and .5.

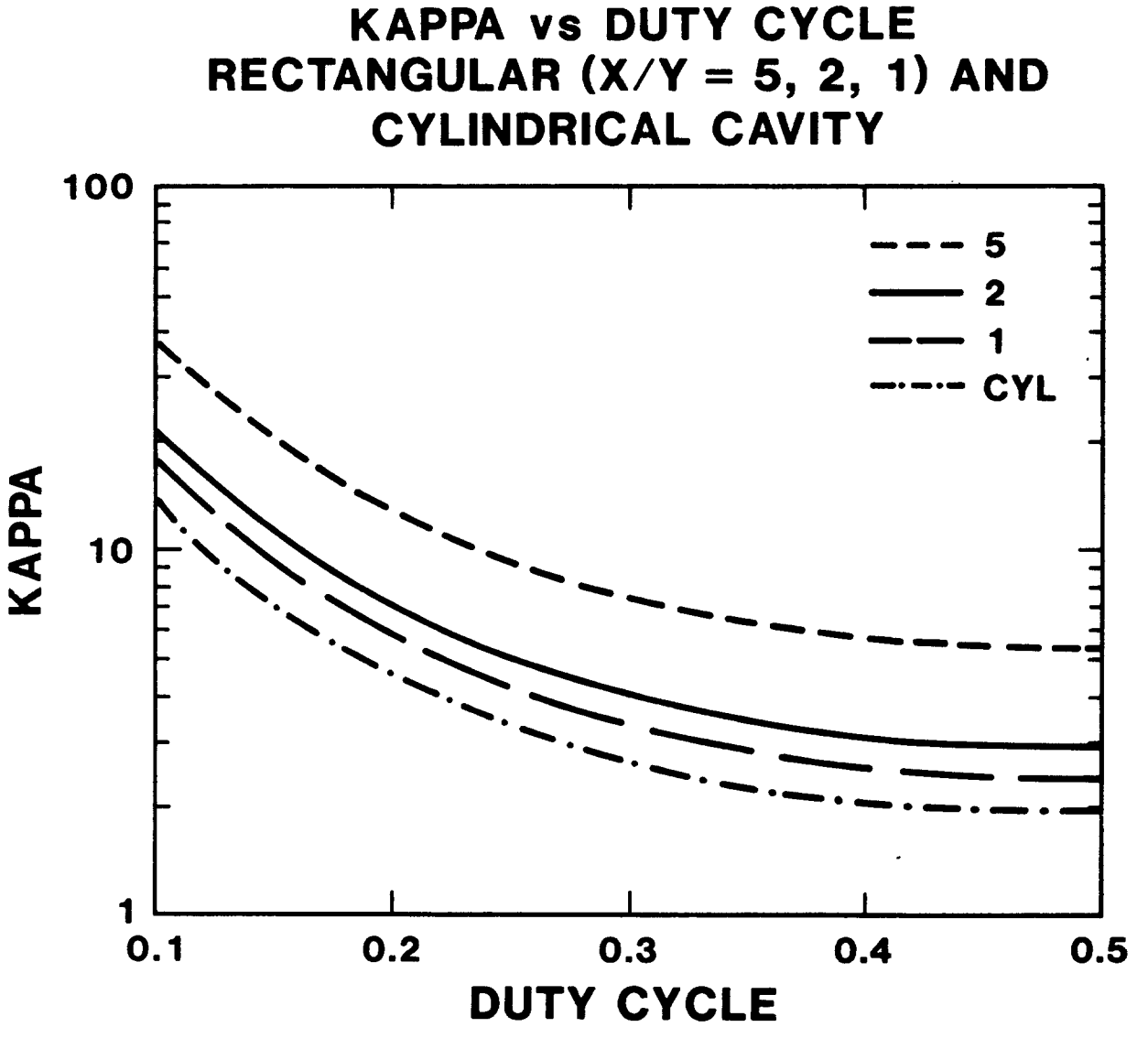

FIGURE 5. κ vs duty cycle for various shaped cavities.

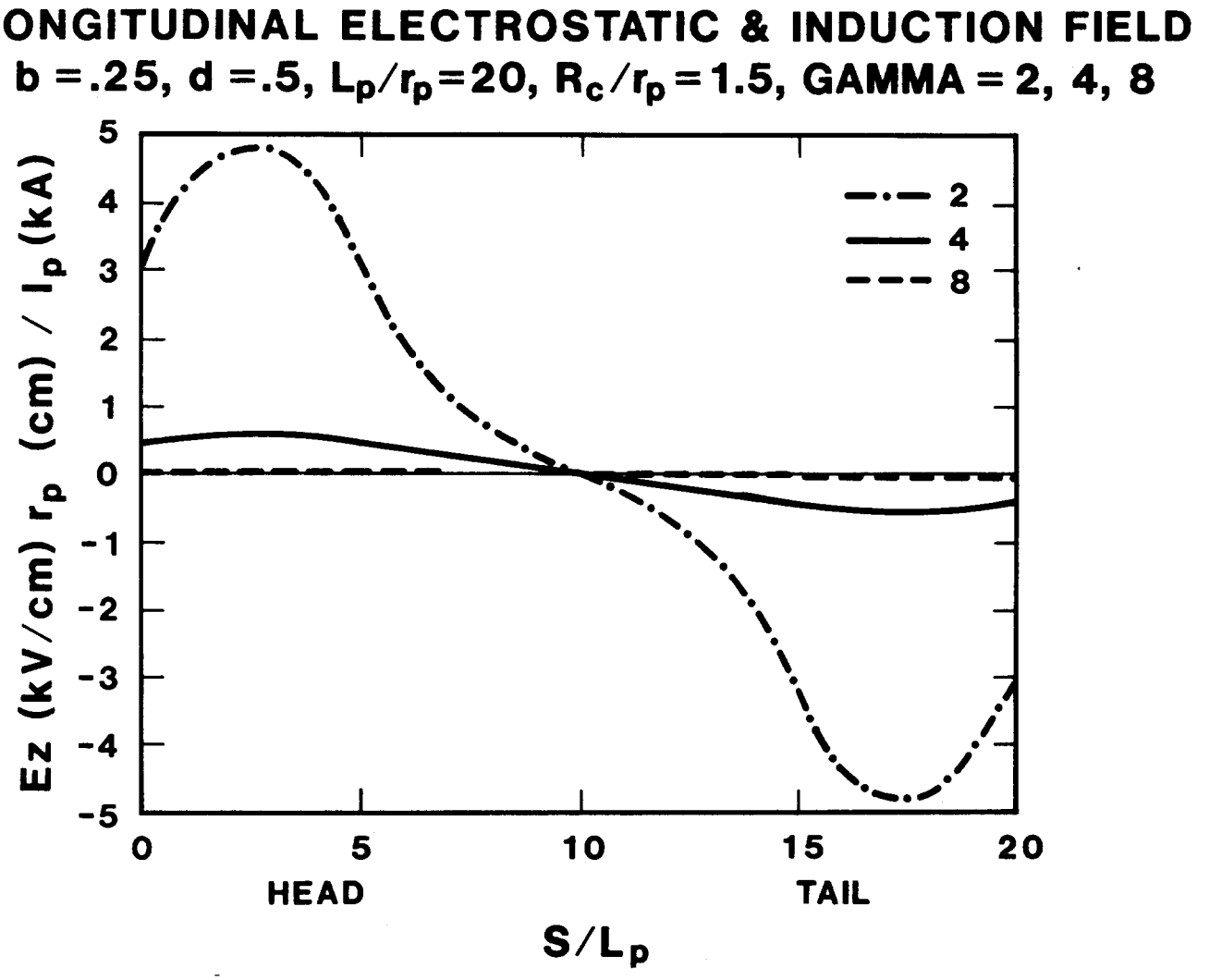

FIGURE 6. Longitudinal electrostatic/inductive field as a function of position for b = .25, d = .5, R_c/r_p = 1.5, L_p/r_p = 20 and a range of γ.

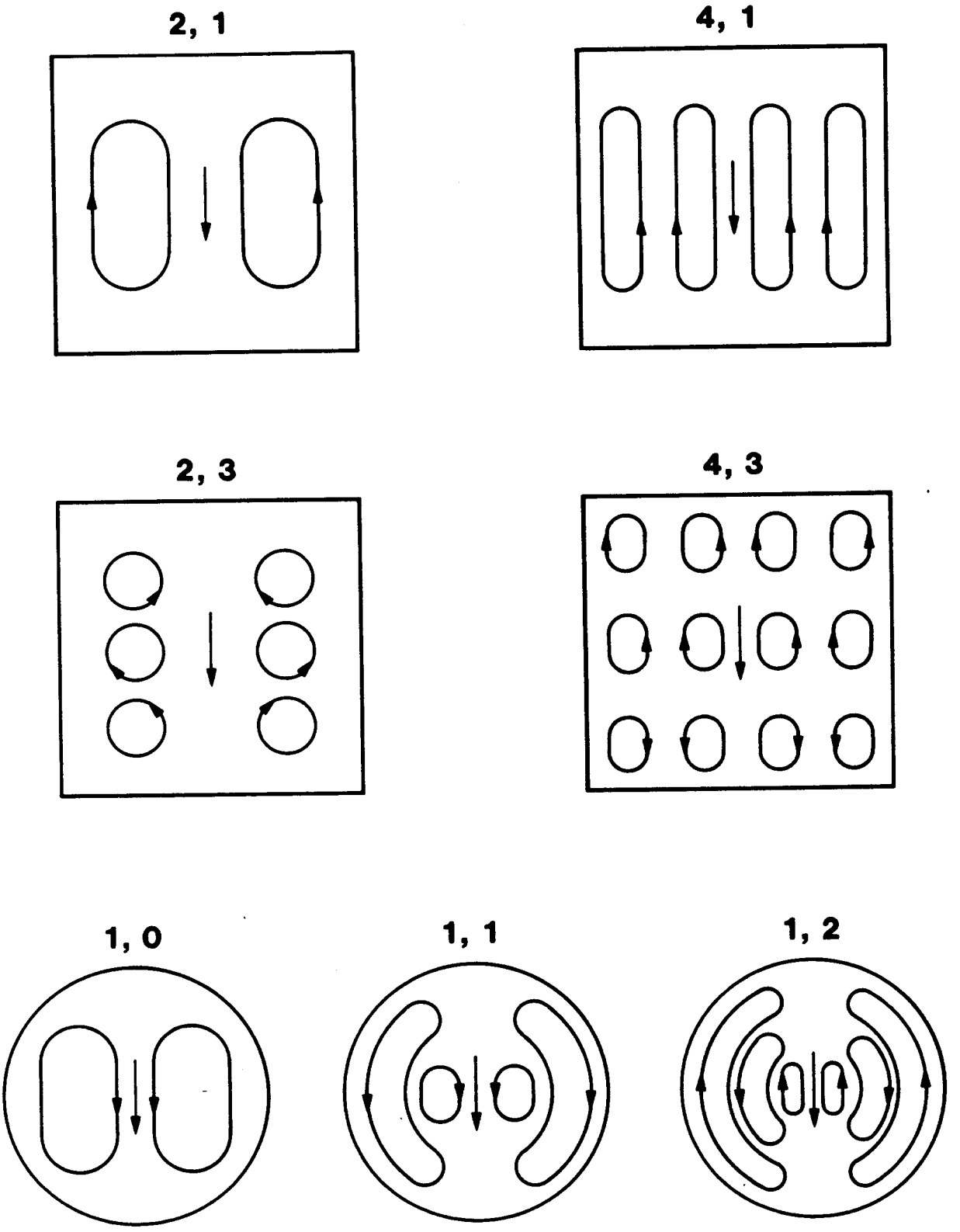

FIGURE 7. Magnetic fields in rectangular and cylindrical cavities.

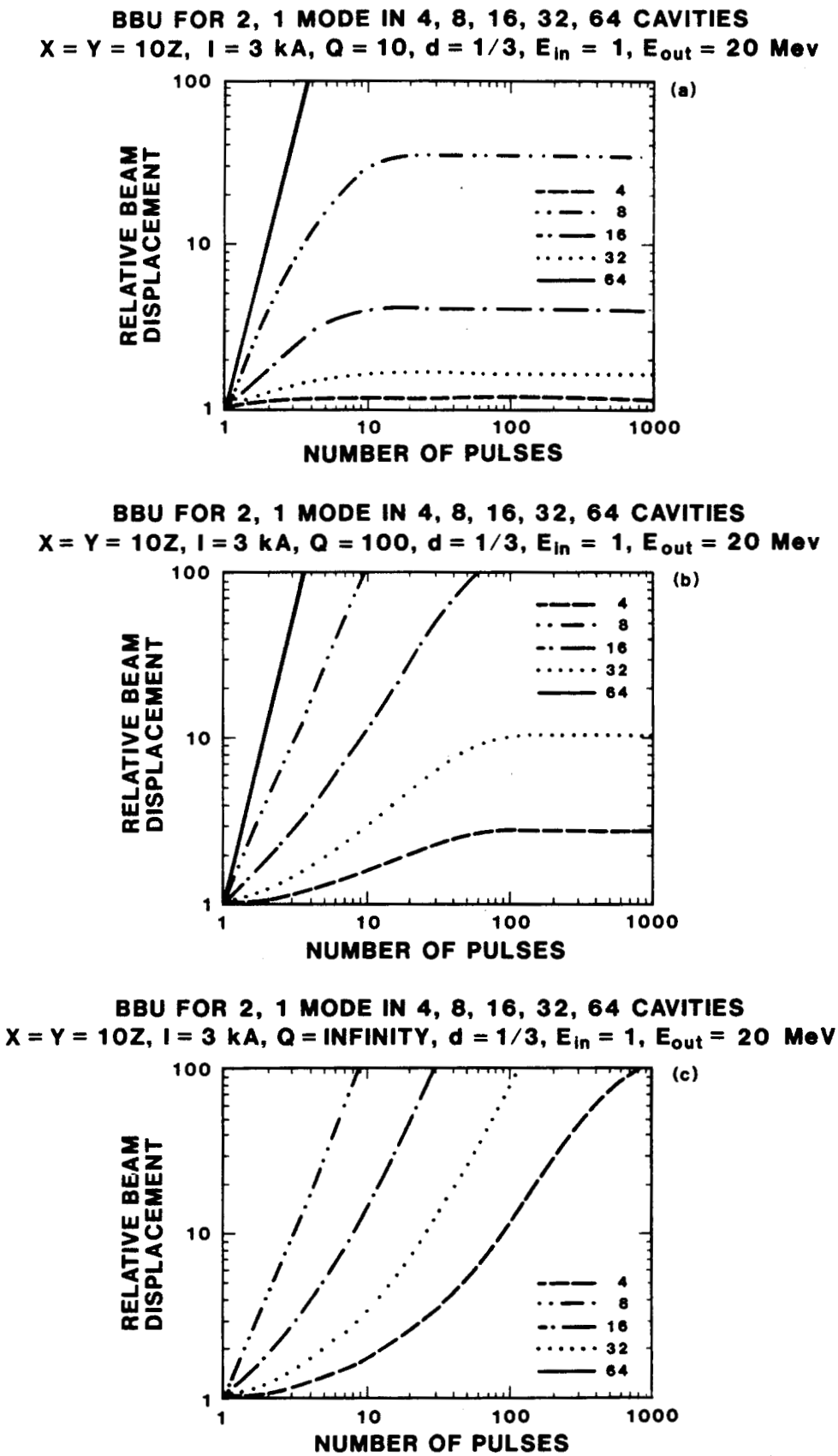

FIGURE 8. BBU Displacement for 3 kA pulse with (a) Q =10, (b) 100, and (c)∞.

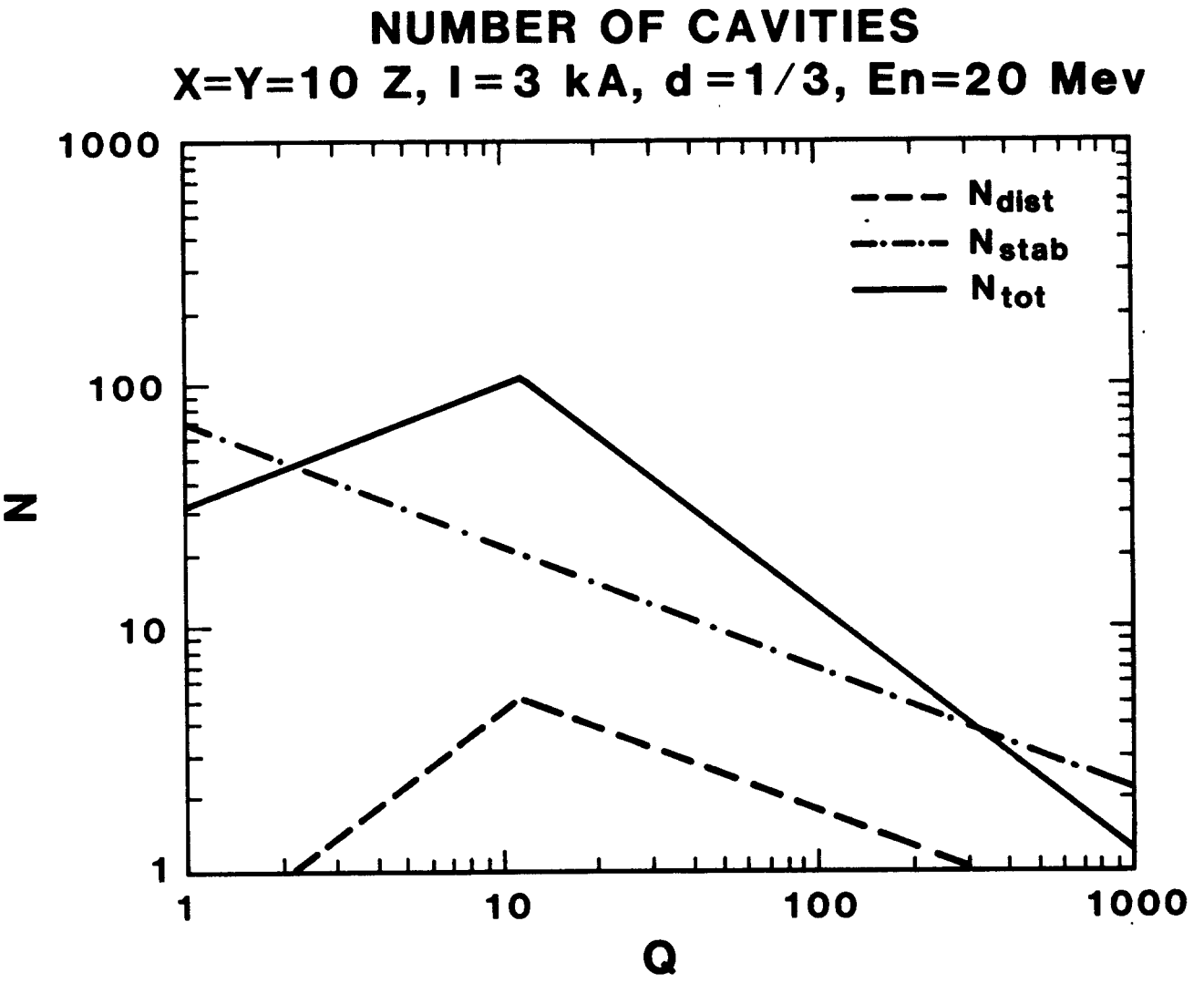

FIGURE 9. N_{dist}, N_{stab}, and N, for a 1 kA, 20 MeV beam with duty cycle 1/3.

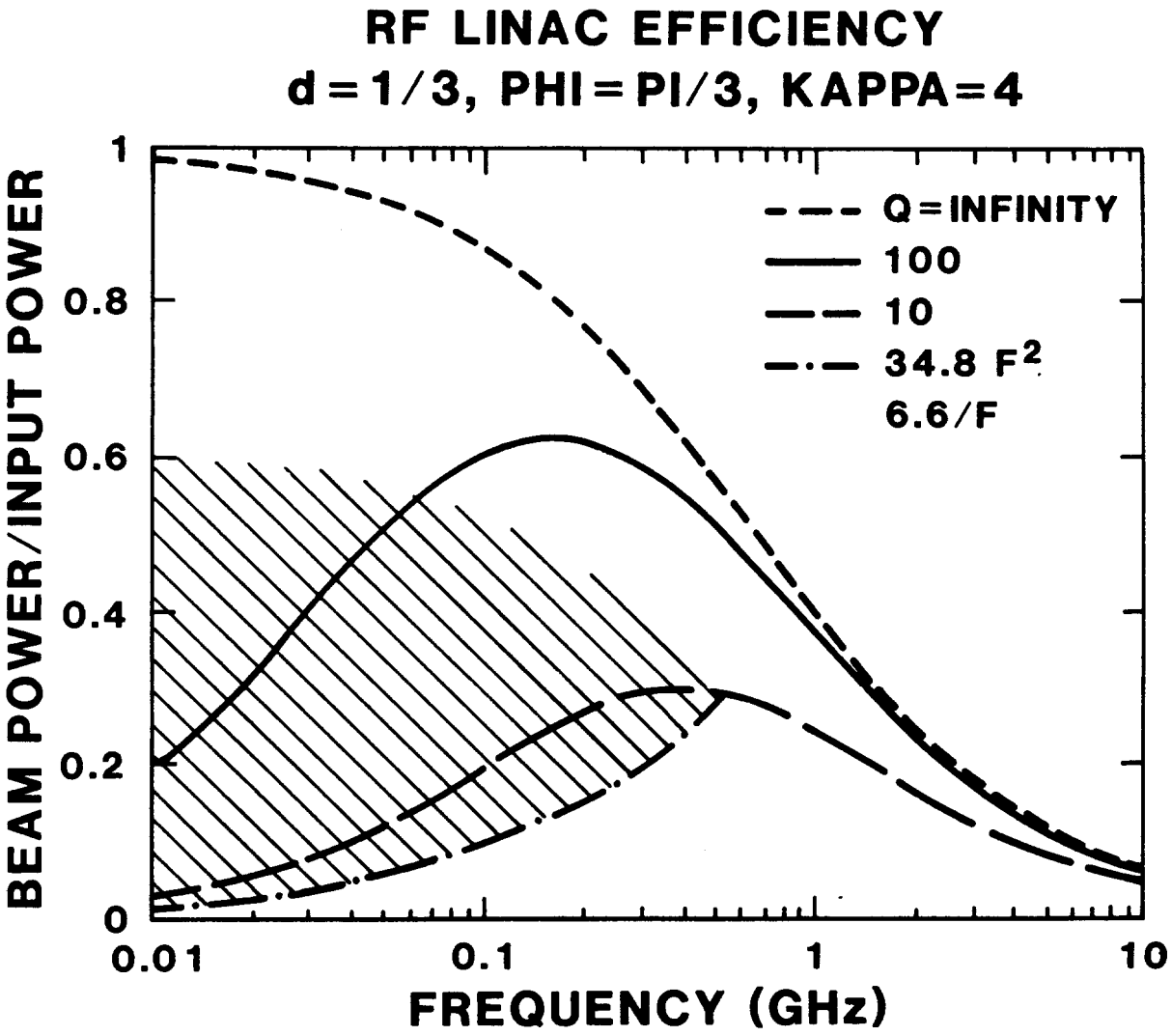

FIGURE 10. Efficiency vs frequency for a 1 kA, 20 MeV beam with duty cycle 1/3 and a range of Q values. Acceptable limits on Q shown by hatched region.

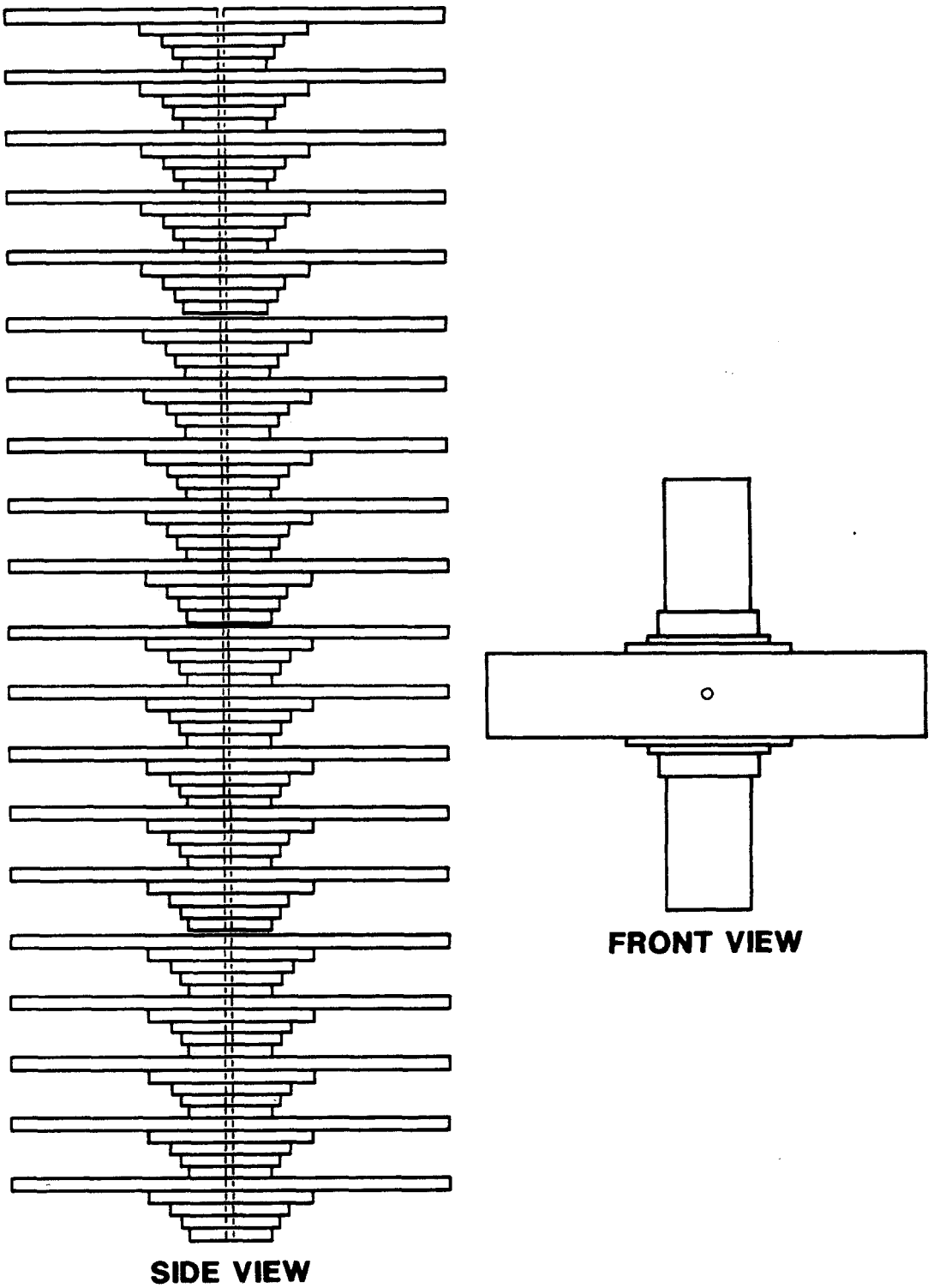

FIGURE 11. Sketch of a 100 cavity accelerator consisting of 20 blocks of 5 distinct cavities.

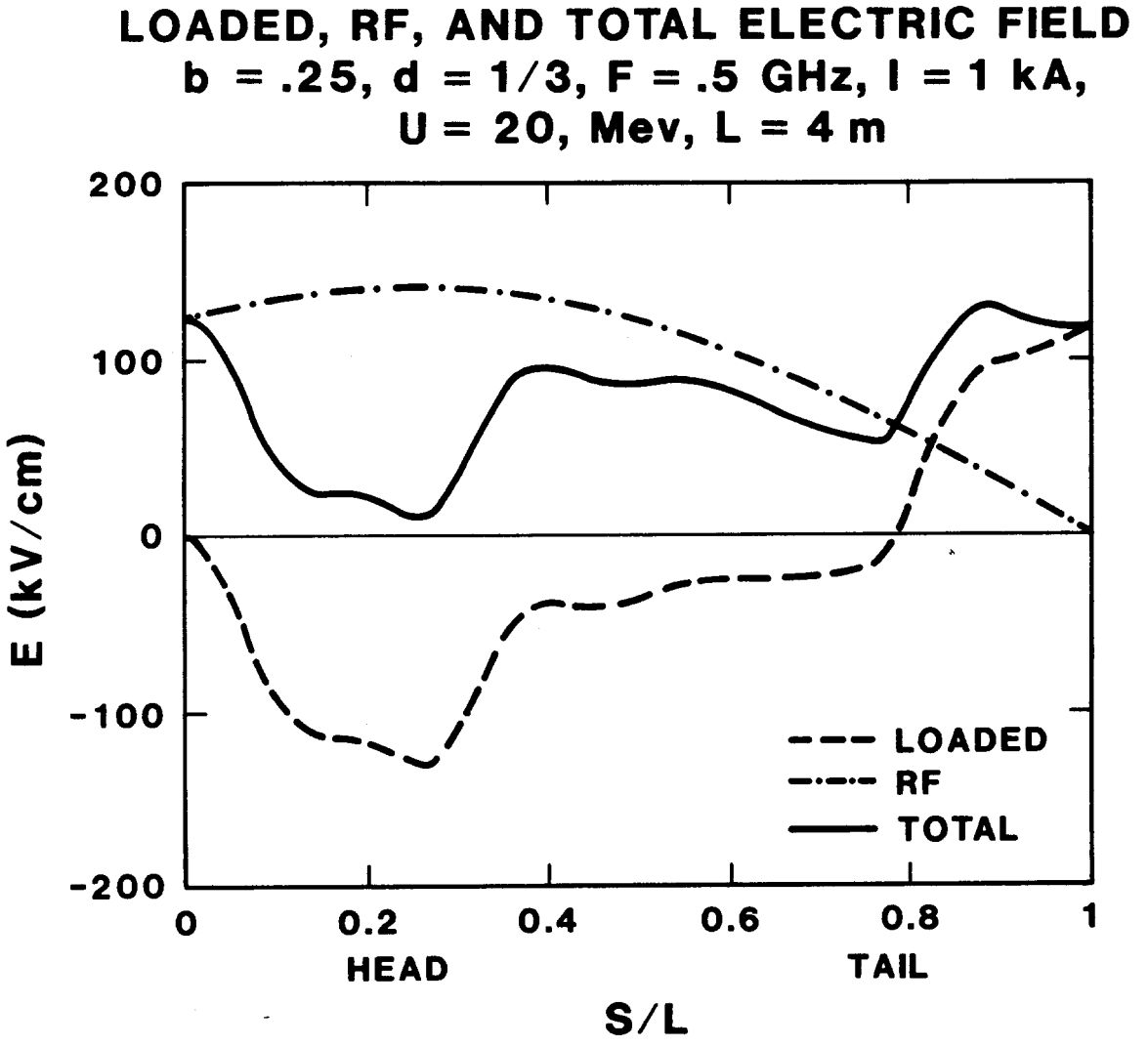

FIGURE 12. Electric field on a pulse with shape factor .25 for 500 MHz source.

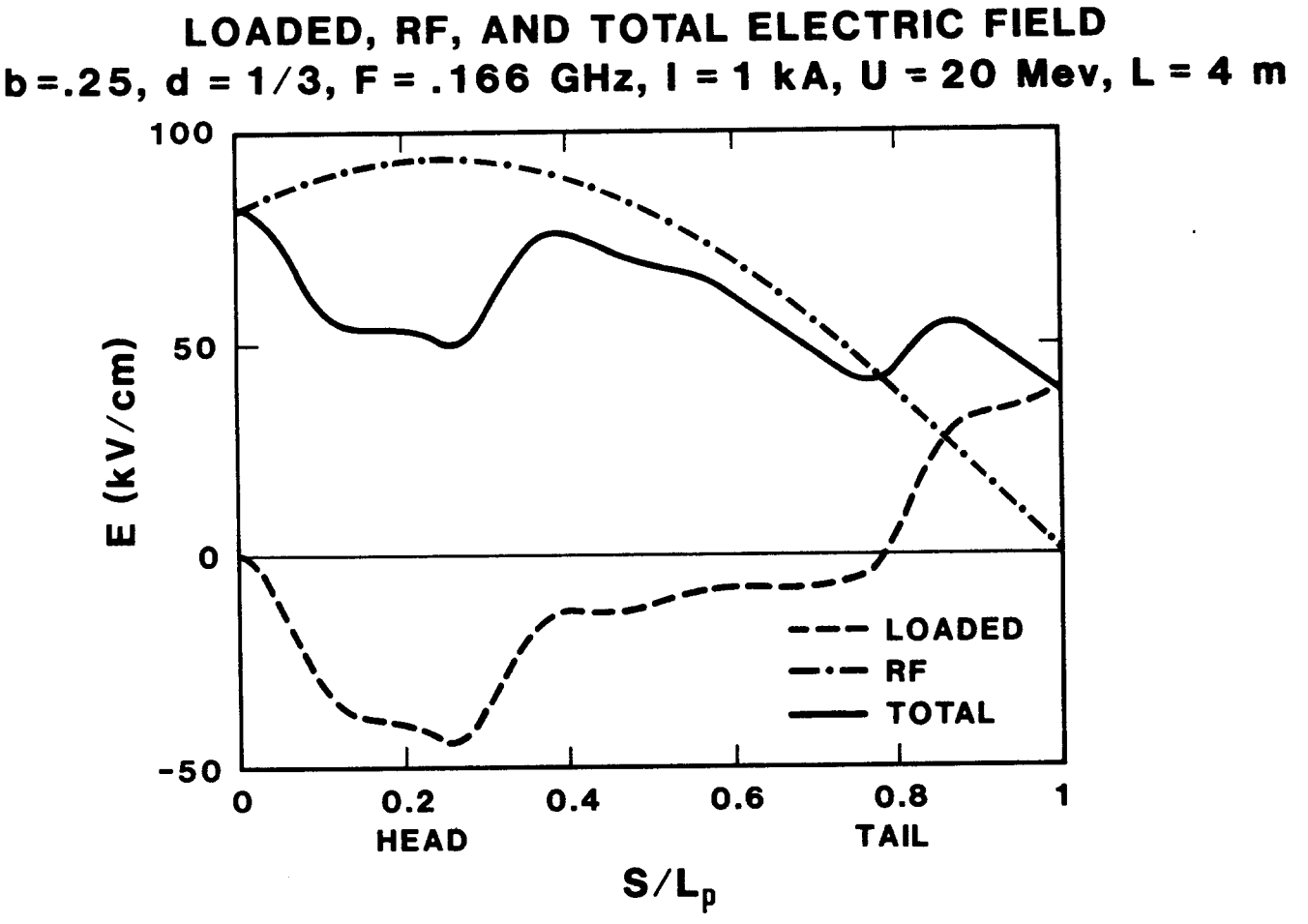

FIGURE 13. As in 14 but with a 166 MHz source.

DISTRIBUTION:
Unlimited Release

Mission Research Corporation
1720 Randolph Road, SE
Albuquerque, NM 87106
Attn: Brendan Godfrey

1000	V. Narayanamurti
1200	J. P. VanDevender
1230	J. E. Powell
1235	J. M. Hoffman
1235	M. C. Clark
1235	L. D. Bacon
1240	K. R. Prestwich
1241	J. R. Freeman + MTS (8)
1241	B. M. Marder (10)
1248	M. T. Buttram
1248	R. W. Stinnett
1261	M. J. Clauser
1270	J. P. VanDevender, Actg. Mgr.
1272	D. E. Hasti
1274	R. J. Lipinski
1274	P. D. Coleman
1274	T. R. Lockner
3141	S. A. Landenberger (5)
3151	W. L. Garner (3)
3154-3	C. H. Dalin for DOE/OSTI (28)
8024	P. W. Dean (1)